

## Supporting Information

# Identifying Sequential Substrate Binding at the Single-Molecule Level by Enzyme Mechanical Stabilization

Jaime Andrés Rivas-Pardo<sup>\*,‡,†</sup>, Jorge Alegre-Cebollada<sup>†</sup>, César A. Ramírez-Sarmiento<sup>‡</sup>,  
Julio M. Fernandez<sup>\*,†</sup> and Victoria Guixé<sup>\*,‡</sup>

<sup>†</sup> Department of Biological Sciences, Columbia University, Northwest Corner Building, 550 West 120 Street, New York, New York 10027, USA.

<sup>‡</sup> Laboratorio de Bioquímica y Biología Molecular, Departamento de Biología, Facultad de Ciencias, Universidad de Chile, Las Palmeras 3425, Casilla 653, Santiago, Chile.

\* Address correspondence to [jar2228@columbia.edu](mailto:jar2228@columbia.edu), [jfernandez@columbia.edu](mailto:jfernandez@columbia.edu), [vguixe@uchile.cl](mailto:vguixe@uchile.cl)

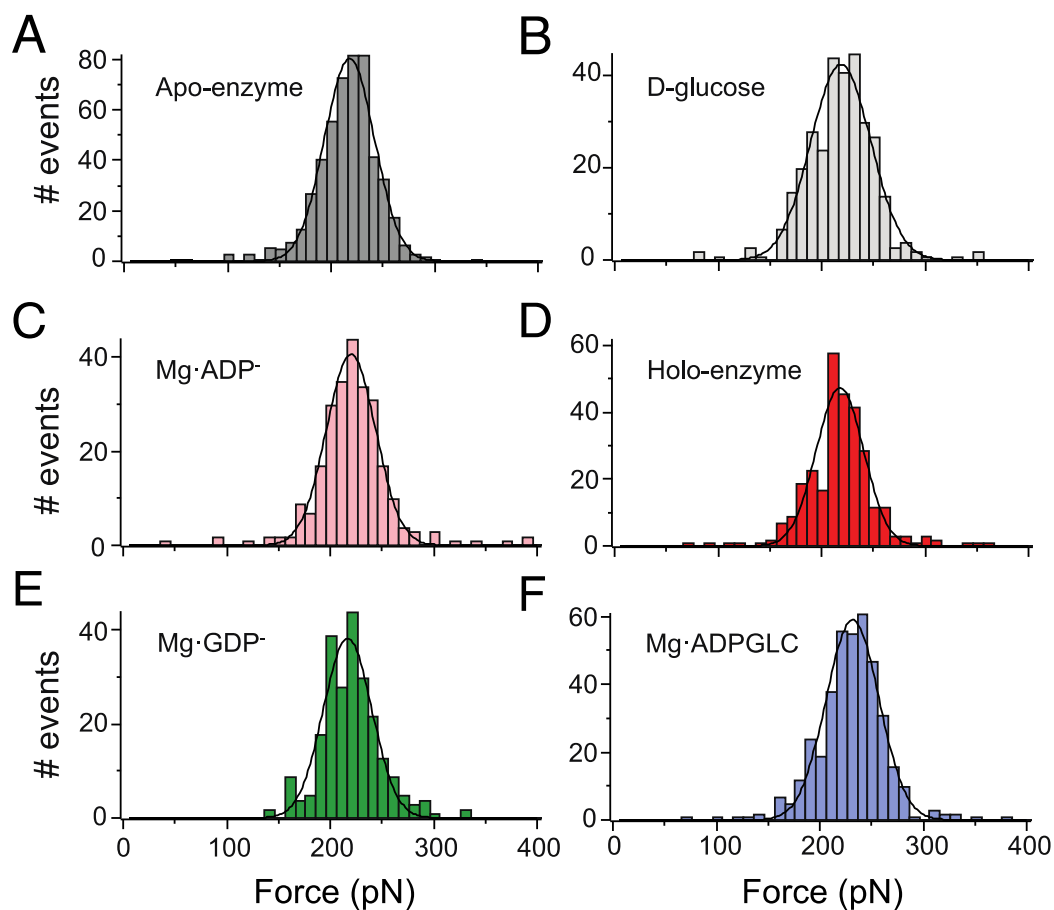


### Figure S1. Mechanical unfolding of the I27 module

Histograms for the unfolding force of I27 module in the absence of substrate (A), in the presence of substrates D-glucose (B), Mg·ADP<sup>-</sup> (C), and Mg·ADPβS·D-glc (D). Also, the inhibitors Mg·GDP<sup>-</sup> (E) and Mg·ADP-GLC (F), are shown. Solid black lines correspond to a Gaussian fit. **Table 3** and **Table S1** summarize all the unfolding forces for the I27 modules under different experimental conditions.

## Statistical errors

Although the data presented along the article consider the mean  $\pm$  s.d. of Gaussians distributions, in Table S1 we showed the unfolding forces in terms of the mean  $\pm$  s.d. of the data collected for each condition.

**Table S1. Mean unfolding forces of  $\Delta L_{C1}$  and  $\Delta L_{C127}$**

	TIGK						I27		
	$\Delta L_{C1}$			$\Delta L_{C1}^*$			Force (pN)	n	(P)
	Force (pN)	n	(P)	Force (pN)	n	(P)			
<b>Apo-enzyme</b>	47 $\pm$ 23	139	<i>reference</i>	N.D.	-	-	210 $\pm$ 41	511	-
<b>D-glucose</b>	49 $\pm$ 23	88	>0.05	N.D.	-	-	211 $\pm$ 34	315	>0.05
<b>Mg·ADP</b>	56 $\pm$ 25	71	<0.05	73 $\pm$ 44	59	<0.01	214 $\pm$ 37	259	>0.05
<b>Holo-enzyme</b>	68 $\pm$ 25	82	<0.001	65 $\pm$ 38	72	<i>reference</i>	213 $\pm$ 36	297	>0.05
<b>Mg·GDP</b>	58 $\pm$ 15	64	<0.05	70 $\pm$ 43	44	<0.01	213 $\pm$ 29	238	>0.05
<b>Mg·ADP·GLC</b>	63 $\pm$ 24	107	<0.001	99 $\pm$ 43	92	<0.01	226 $\pm$ 43	401	>0.05

The forces reported in the table are the mean value  $\pm$  standard deviation of the data. Statistical analysis was made using one-way Anova. *P* values in the table are considering apo-condition as reference ( $\Delta L_{C1}$ ) or holo-enzyme ( $\Delta L_{C1}^*$ )

## Binding of D-glucose to TIGK

The individual addition of the substrates does not change the fluorescence intensity of any of the four Trp residues present in the TIGK (positions: Trp<sup>12</sup>, Trp<sup>97</sup>, Trp<sup>111</sup> and Trp<sup>113</sup>) (**Figure S2A**). However, we measured the effect of D-glucose in the presence of the Mg·AMP complex (product the reaction), observing increments in the intensity respect to increments in the concentration of D-glucose (**Figure S2B**). This result shows that D-glucose and the nucleotide trigger a major conformational arrangement, which should change the microenvironment of the Trp residues of the enzyme. D-glucose by itself is not able to triggers such change, suggesting absence of binding to the enzyme. In summary, our results indicate that the binding of D-glucose in the absence of the nucleotide is very unlikely.

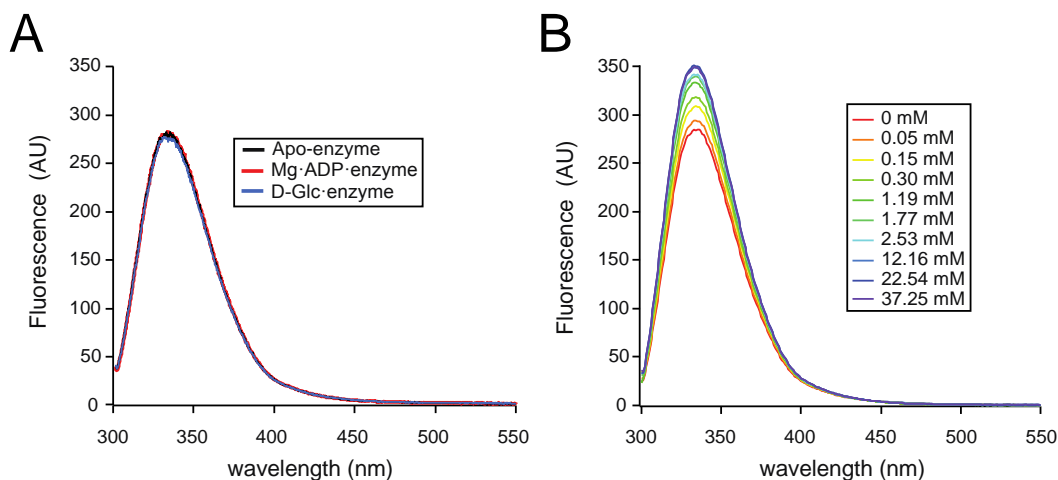


**Figure S2. Binding of D-glucose occurs only in the presence of the nucleotide.**

(A) Emission spectrum of TIGK recorded upon excitation at 295 nm. After the addition of 5 mM Mg·ADP or 10 mM D-glucose, the fluorescence intensity does not change. (B) Fluorescence intensity change by addition of D-glucose (0 mM – 37.25 mM) in the presence of 5 mM Mg·AMP. The experiments were recording at 313 K using an excitation and emission slit of 3 nm.

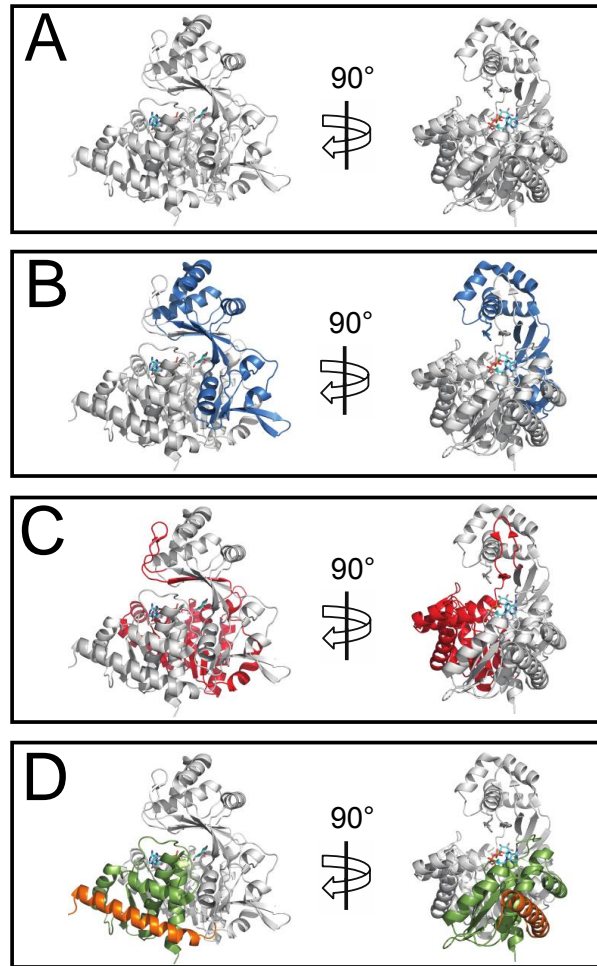


**Figure S3. Mechanical intermediates present in TIGK**

(A) Cartoon representation of TIGK (PDB ID 4B8S). In (B) and (C) presumed mechanical intermediates 1 and 1\* are highlight in the structure in blue and red, respectively. In (B), the intermediate includes from Asp40 ( $\beta$ 2) to Asp190 ( $\beta$ 8), capturing ~150 residues between the two  $\beta$ -strands. On the other hand, the intermediate in (C) is formed between Val33 to Tyr37 ( $\beta$ 1) + Pro191 to Thr353, around 166 residues in total. (D) Shows the secondary structure that presumably is not detected during the force extension experiments. The  $\alpha$ 1 is highlighted in orange (residues 1 to 32), whereas the structure between  $\beta$ 14 and  $\alpha$ 17 in green (residues 357 to 467). The ADP and D-glucose are represented in sticks. The  $\beta$ -phosphate of ADP has been included for representation purposes (PDB ID 1GC5).

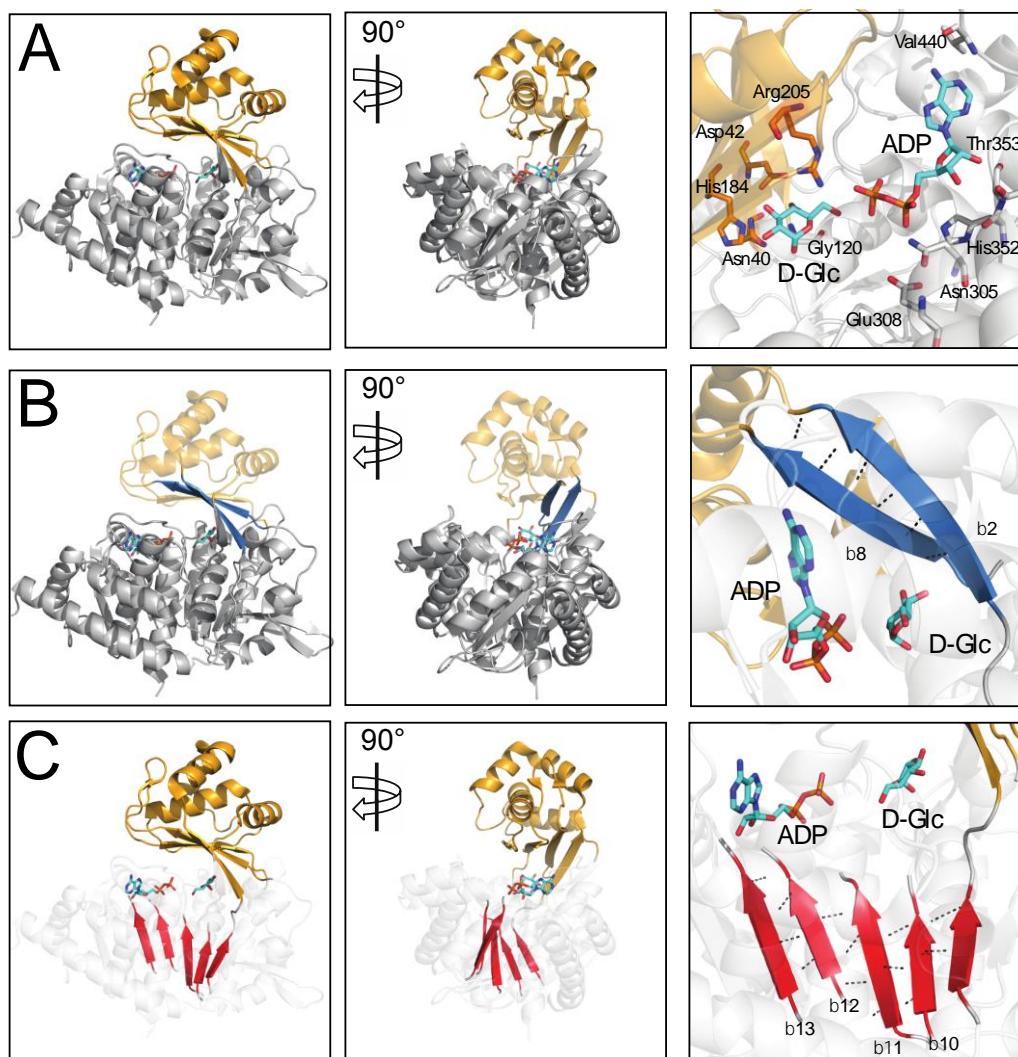


**Figure S4. Crystal structure of TIGK and mechanical clamps**

In (A) the crystal structure of the enzyme is shown (PDB ID 4B8S). The small domain is represented in yellow, whereas the large domain in gray (left and center). The binding site is located between both domains (right). (B) and (C) show possible locations of the mechanical clamps present in the intermediates 1 and 1\*, respectively. The mechanical clamp in  $\Delta L_{C1}$  is in the small domain (B), in  $\beta$  strands 2 and 8 (in blue) (B, right panel). The mechanical clamp in  $\Delta L_{C1^*}$  is in the large domain (C), between  $\beta$  strands  $\beta 1$ - $\beta 10$ - $\beta 11$ - $\beta 12$ - $\beta 13$  (in red) (C, right panel). Both mechanical intermediates, offer several H-bonds to the ADP and D-glucose. The ADP and D-glucose are represented in sticks. The  $\beta$ -phosphate of ADP has been included for representation purposes (PDB ID 1GC5).